Supporting Information

Sensitive colorimetric sensor for point-of-care detection of acetylcholinesterase using cobalt oxyhydroxide nanoflakes

Rui Jin [a]†, Zihao Xing [b]†, Deshuai Kong [a], Xu Yan [a,]*, Fangmeng Liu [a], Yuan Gao [a], Peng Sun [a], Xishuang Liang [a], Geyu Lu [a,]*

[a] *State Key Laboratory on Integrated Optoelectronics, Jilin Key Laboratory on Advanced Gas Sensor, College of Electronic Science and Engineering, Jilin University, Changchun 130012, People's Republic of China*

[b] *State Key Laboratory of Inorganic Synthesis and Preparative Chemistry, College of Chemistry, Jilin University, Changchun 130012, People's Republic of China*

†These authors (R. Jin and Z. H. Xing) contributed equally to this work.

The authors declare no competing financial interest.

***Corresponding Author**

E-mail Address: yanx@jlu.edu.cn (X. Yan)

E-mail Address: lugy@jlu.edu.cn (G.Y. Lu)

1. The synthesis of Au NCs and Fe_3O_4 NPs

Synthesis of Fe_3O_4 NPs [S1]: $FeCl_3 \cdot 6H_2O$, $FeCl_2 \cdot 4H_2O$ and HCl were dissolved in 15 mL deionized water to prepare a stock solution. Then the stock solution was added into NaOH solution under nitrogen gas protection with the solution vigorously stirred at 80 ℃. The obtained Fe_3O_4 nanoparticles washed with deionized water four times.

Synthesis of Au NCs [S2]: $HAuCl_4$ was added to BSA under vigorous stirring. NaOH was introduced 2 min later, and the reaction was under vigorous stirring for 12 h. The as-synthesized Au NCs were purified through continuous ultrafiltration using a 3000 MW filter under centrifugation.

The concentration of nanomaterials was determined by the following steps: the synthesized nanomaterials were freeze-dried, then 2.5 mg of the materials were weighed and dissolved in 5.0 mL of deionized water. Finally, the concentration of Au NCs and Fe_3O_4 NPs were 500 μg mL^{-1}.

2. Kinetic analysis

The apparent steady-state kinetic parameters for the catalytic oxidation of substrates by CoOOH NFs, using the Beer-Lambert Law at kinetics mode of UV-vis spectrophotometer (UV-2550). Kinetic experiments carried out using of CoOOH NFs (270 μmol L^{-1}) in acetate buffer (0.1 mol L^{-1}, pH 4.5) which containing 1 mmol L^{-1} H_2O_2 as substrate, and various concentration of TMB (0.01-0.3 mmol L^{-1}). In addition, the kinetics at variable H_2O_2 concentrations (0.05-20 mmol L^{-1}) with a constant TMB concentration (0.3 mmol L^{-1}) was also investigated.

3. Colorimetric detection of H_2O_2

The colorimetric assay was carried out as follows: 150 μL CoOOH NFs (25 μg mL^{-1}) and 50 μL TMB (1 mg mL^{-1}) and 200 μL acetate buffer solution (0.1 mol L^{-1}, pH 4.0) with 1000 μL water, then adding different concentrations of H_2O_2 (100 μL) solution. The mixture was incubated for 15 min at room temperature. Finally, the color absorbance at 652 nm was recorded.

4. Measurement of AChE inhibitor

Parathion-methyl (PM) as a traditional AChE inhibitor produced a reduced color intensity by the AChE-CHO@CoOOH (ACh) system. Different concentrations of 25 μL PM and 25 μL of AChE (1.0 U mL^{-1}) were mixed at 37°C for 30 min. Then 50 μL ACh (50 mmol L^{-1}), 50 μL CHO (2.0 U mL^{-1}) and 50 μL Tris–HCl buffer (0.1 mol L^{-1}, pH 7.5) were added at 37°C for

another 30 min. Subsequently, 150 μL of CoOOH NFs (25 μg mL^{-1}), 50 μL of TMB solution (1.0 mg mL^{-1}), 200 μL acetate buffer (0.1 mol L^{-1}, pH 4.0) and 950 μL of deionized water were diluted to 1500 μL. After 5 min, the absorbance of the mixture at 652 nm was collected.

5. Real sample detection

The present colorimetric assay was employed to detect AChE in human serum in order to evaluate its applicability. A healthy human serum was provided kindly by Jilin University School Hospital (Changchun, China). The experiment carried out in accordance with the relevant laws and institutional guidelines. Some of the pretreatments were taken to eliminate the interference of coexisting substances because of the high protein in the blood plasma. The processing steps were as follows: 1 mL of human serum and 2 mL of deionized distilled water mixed with 2 mL of acetonitrile via vortexing for 5 min. Subsequently, the human serum sample was deproteinized by adding 5 mL of 10% (w/v) trichloroacetic acid. Finally, the serum solution was acquired by centrifuging (10,000 rpm, 15 min) to remove the protein and other macromolecules precipitate. The supernatant serum samples were diluted 10-fold with deionized distilled water and applied to measure AChE according the mentioned process. For recovery study, certain amounts of AChE standard were spiked into the samples before any pretreatments evaluated by described procedure.

6. Data analysis

We use the inhibition efficiency (IE %) of AChE as reaction signal for the analysis of PM. IE % was analyzed by the following equation (1):

$$IE\ \% = (F_{inhibitor} - F_{no\ inhibitor}) / (F_0 - F_{no\ inhibitor}) \times 100\% \quad (1)$$

Where $F_{inhibitor}$ and $F_{no\ inhibitor}$ represent the absorbance intensity of AChE-CoOOH-TMB system and AChE-CoOOH-TMB-PM system, respectively. F_0 refers to the absorbance intensity of the CoOOH-TMB system without AChE and methyl parathion.

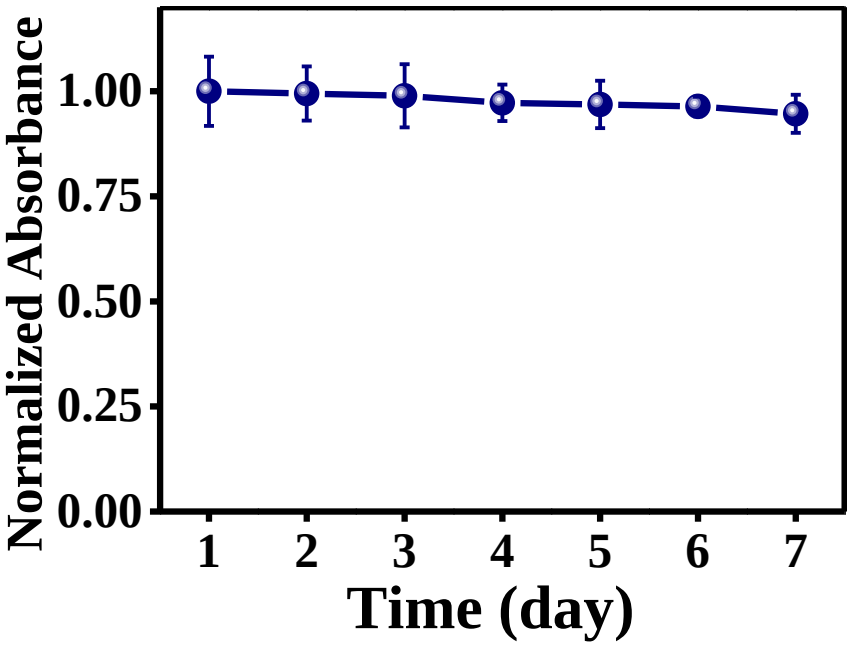

Fig. S1. The stability of CoOOH NFs peroxidase-like activity in seven days.

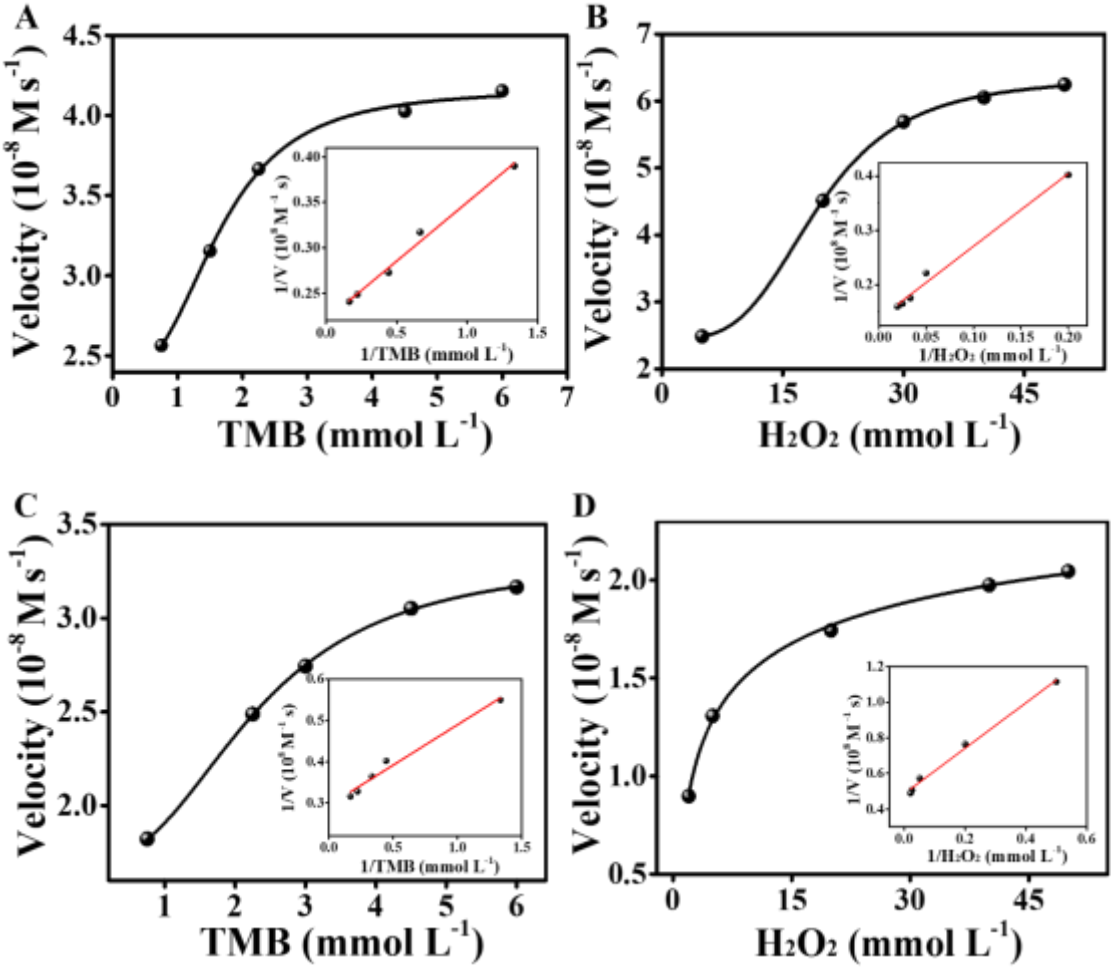

Fig. S2. Steady-state kinetic analyses using the Michaelis−Menten model and Lineweaver−Burk model (insets) for Fe_3O_4 NPs (A and B) and Au NCs (C and D).

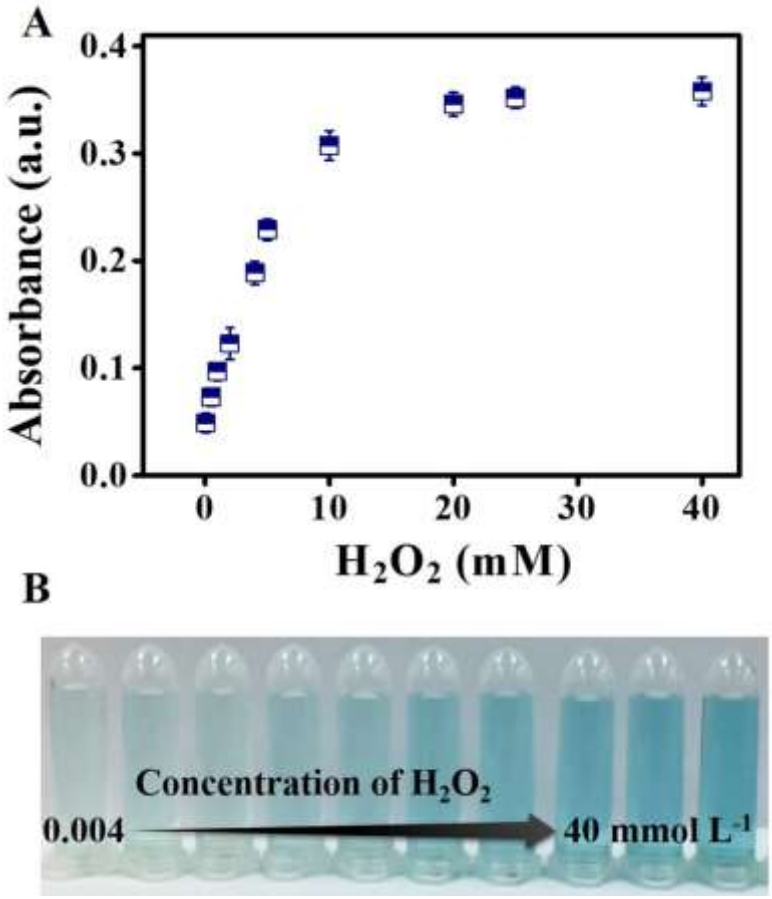

Fig. S3. (A) The UV-Visible absorption spectra of the reaction solutions containing 25 μg mL^{-1} CoOOH nanoflakes with different concentration of H_2O_2 (from 0.004 to 40 mmol L^{-1}). (B) The corresponding photographs of reaction mixtures after adding different concentrations of H_2O_2.

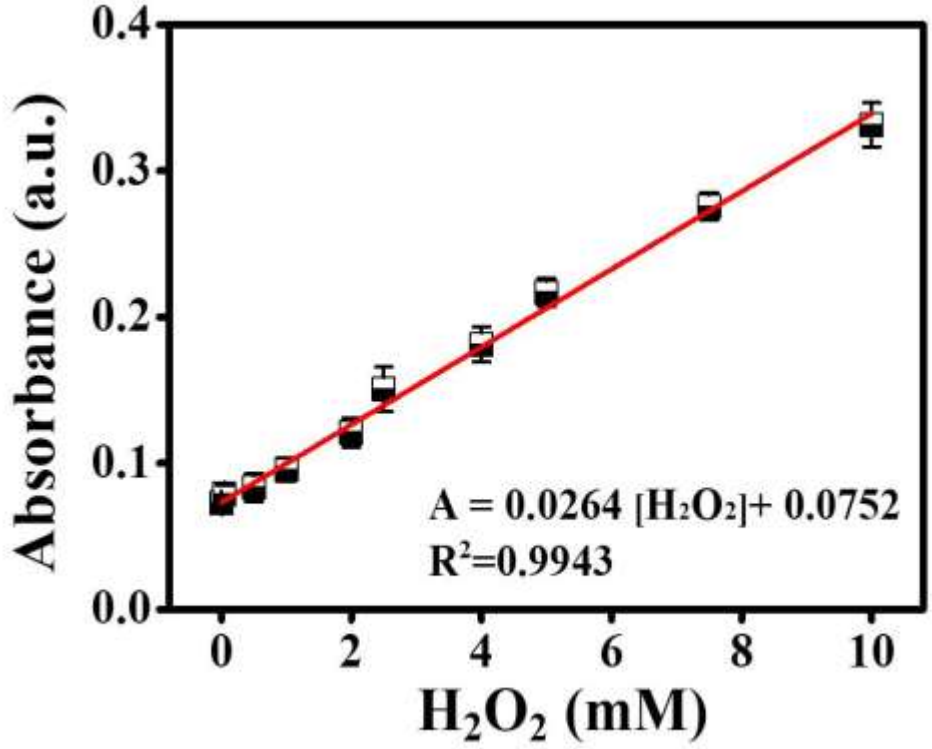

Fig. S4. The linear calibration plot of absorbance at 652 nm versus H_2O_2 concentrations. The error bars represent the standard deviation across three repeated assays.

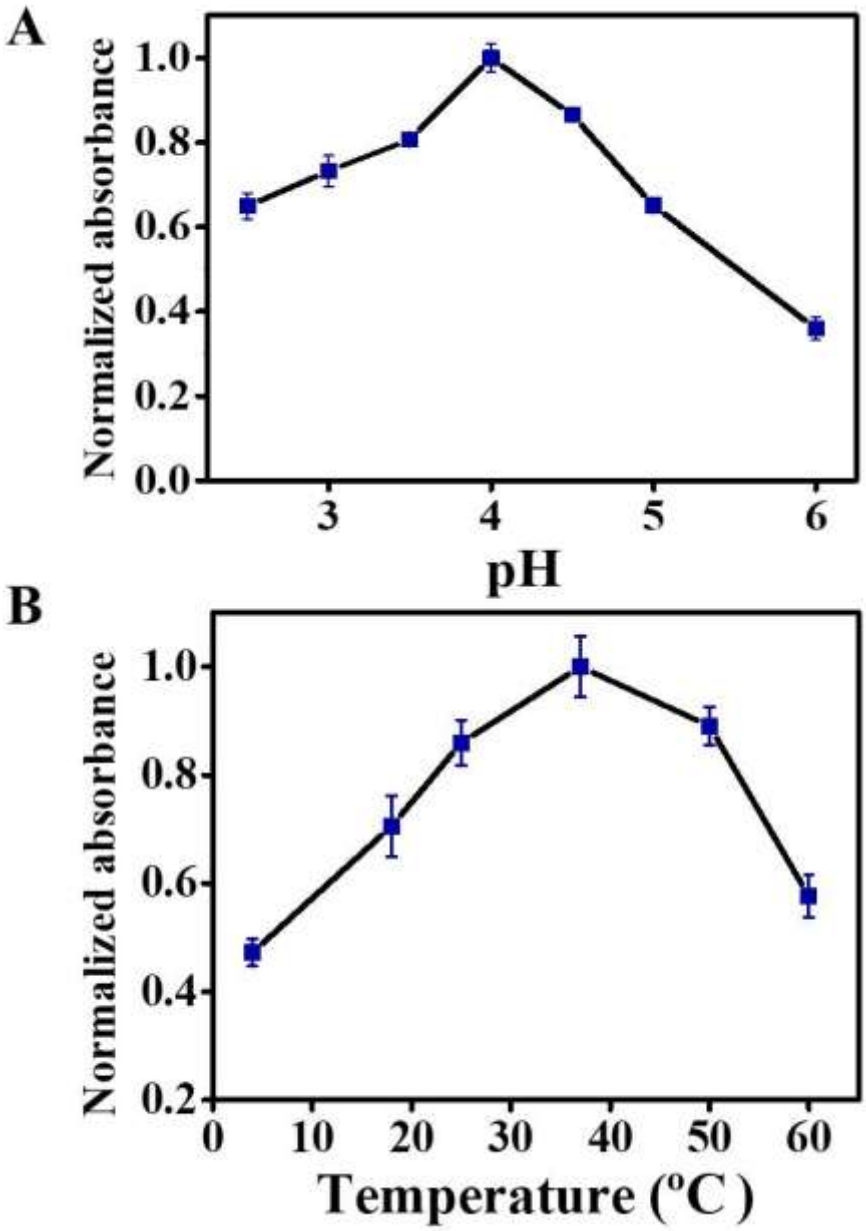

Fig. S5. Effect of reaction pH (A) and temperature (B) on TMB oxidation by H_2O_2 in the presence of CoOOH nanoflakes. The maximum value observed during each test was set as 100%, and the normalized absorbance measured at each condition was plotted against. The samples contained 25 μg mL^{-1} CoOOH nanoflakes, 15 mmol L^{-1} H_2O_2, 1 mg mL^{-1} TMB, and 0.1 mol L^{-1} NaAC buffer. The error bar represents the confidence interval for the mean of three measurements.

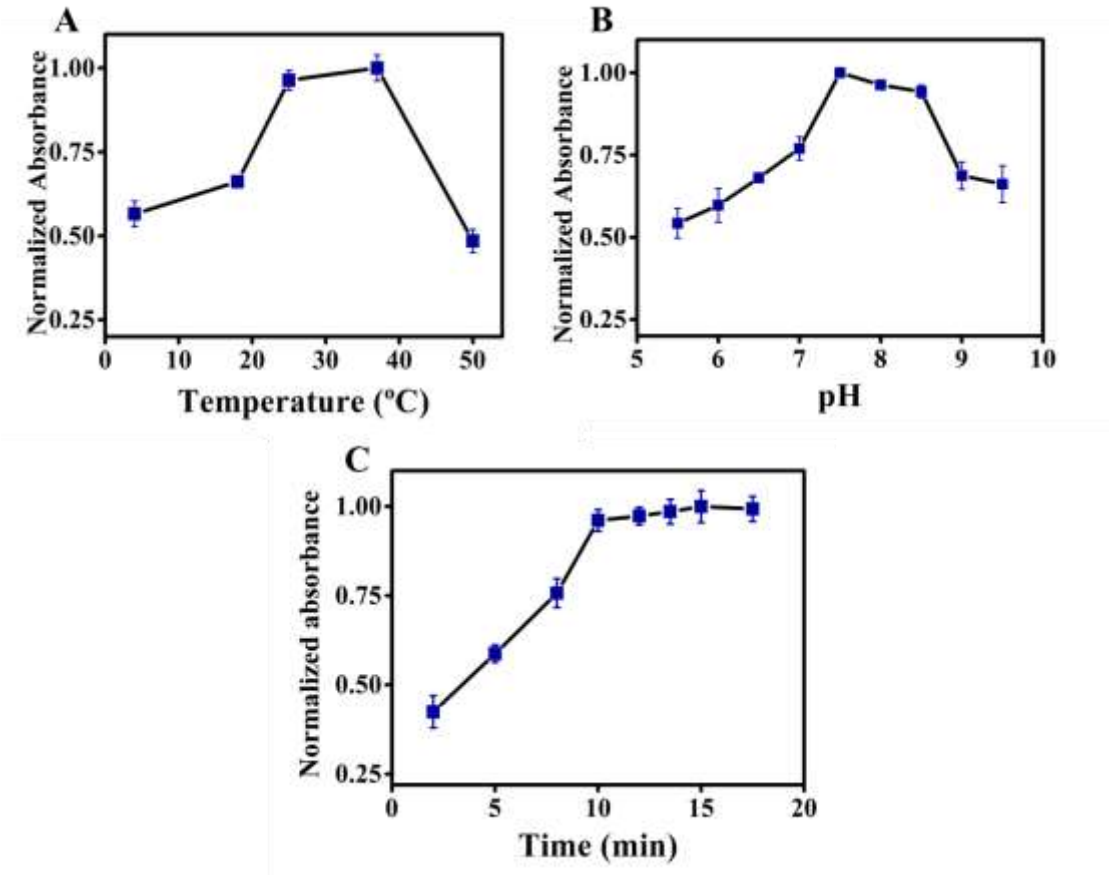

Fig. S6. Optimization of the reaction temperature, pH and time. The maximum value observed during each test was set as 100%, and the normalized absorbance measured at each condition was plotted against. The samples contained 25 μg mL^{-1} CoOOH nanoflakes, 50 mmol L^{-1} ACh, 1 U mL^{-1} AChE, 2 U mL^{-1} CHO, 1 mg mL^{-1} TMB, and 0.1 mol L^{-1} NaAC buffer. The error bar represents the confidence interval for the mean of three measurements.

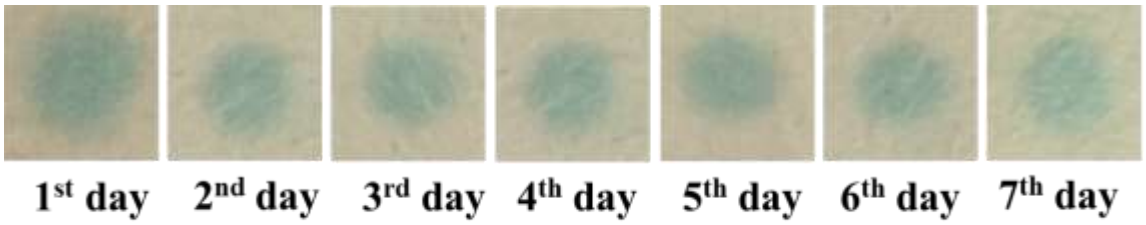

Fig. S7. The stability of paper-based biosensor in seven days.

Table S1. Comparison of the apparent Michaelis-Menten constant (K_m) and maximum reaction rate (V_m).

Catalyst	K_m (mM)		V_m (10^{-8} M s^{-1})	
	H_2O_2	TMB	H_2O_2	TMB
HRP	3.70	0.43	8.71	10.00
CoOOH NFs	0.12	0.98	8.27	5.79
Au NCs	12.55	0.212	2.00	3.30
Fe_3O_4 NPs	9.55	0.591	6.24	4.54

Table S2. Comparison of the detection limit (LOD) for AChE activity using different nanomaterials.

Materials	Linear range (mU mL^{-1})	LOD (mU mL^{-1})	Method	Ref.
MnO_2 NFs	0.01-15	0.035	Colorimetry	S3
Carbon dots	14.2-121.8	4.25	Fluorimetry	S4
Polythiophene-derivative	/	0.2	Colorimetry	S5
Au NCs	0.05-2.0	0.05	Fluorimetry	S6
FITC/BSA-Au NCs	0.11-2.78	0.05	Fluorimetry	S7
Carbon quantum dots	0.05-2.0	0.05	Fluorimetry	S8
Polymer@Photonic nanostructure	10-1000	5	Photonic assay	S9
Protein-Au NCs	14.2-121.8	4.25	Fluorimetry	S10
CoOOH NFs	0.05-20	0.033	Colorimetry	This work

References

S1 A. L. Morel, S. I. Nikitenko, K. Gionnet, A. Wattiaux, J. L. K. Him, C. Labrugere, B. Chevalier, G. Deleris, C. Petibois, A. Brisson and M. Simonoff, *ACS nano,* 2008, **2**, 847–856.

S2 P. Zhao, K. Y. He, Y. T. Han, Z. Zhang, M. Z. Yu, H. H. Wang, Y. Huang, Z. Nie and S. Z. Yao, *Anal. Chem.*, 2015, **87**, 9998–10005.

S3 X. Yan, Y. Song, X. L. Wu, C. Z. Zhu, X. G. Su, D. Du and Y. H. Lin, *Nanoscale,* 2017, **9**, 2317–2323.

S4 Z. Qian, L. Chai, C. Tang, Y. Huang, J. Chen and H. Feng, *Sens. Actuators, B,* 2016, **222**, 879–886.

S5 Y. Li, H. Bai, C. Li and G. Shi, *ACS Appl. Mater. Inter.*, 2011, **3**, 1306–1310.

S6 C. Ke, Y. Wu and W. T. Seng, *Biosens. Bioelectron.,* 2015, **69**, 46–53.

S7 P. J. Ni, Y. J. Sun, S. Jiang, W. D. Lu, Y. L. Wang and Z. Li, *Sens. Actuators, B,* 2017, **240**, 651–656.

S8 W. Li, W. Li, Y. Hu, Y. Xia, Q. Shen and Z. Nie, *Biosens. Bioelectron.,* 2013, **47**, 345–349.

S9 T. Tian, X. S. Li, J. C. Cui, J. Li, Y. Lan, C. Wang, M. Zhang, H. Wang and G. T. Li, *ACS Appl. Mater. Inter.,* 2014, **6**, 15456–15465.

S10 Z. Qian, L. Chai, C. Tang, Y. Huang, J. Chen and H. Feng, *Sens. Actuators, B,* 2016, **222**, 879–886.